

Article

Investigating the Impact of Weather Conditions on Urban Heat Island Development in the Subtropical City of Hong Kong

Yingsheng Zheng^{1,2,3} , Wenjie Li¹, Can Fang¹, Biyin Feng¹, Qiru Zhong¹ and Dongxu Zhang^{1,*}¹ College of Architecture and Urban Planning, Guangzhou University, Guangzhou 510006, China² State Key Laboratory of Green Building in Western China, Xi'an University of Architecture & Technology, Xi'an 710055, China³ School of Architecture, The Chinese University of Hong Kong, Hong Kong SAR 518172, China

* Correspondence: zhangdongxu@gzhu.edu.cn

Abstract: Subtropical monsoon climates, high-density and heterogeneous urban built environments, as well as coastal–mountainous geographical environments influence the development of urban heat island (UHI) effects in Hong Kong. For better weather control of in situ observations and spatial analysis of UHI effects, it is necessary to quantitatively understand the influence of weather conditions on UHI development in Hong Kong and establish weather-based UHI estimation models. Meteorological records of four urban stations, one rural reference station, and one wind reference station at an hourly interval during the period of 2002–2012 were collected from Hong Kong observatory. A frequency analysis of the mean values of multiple meteorological elements and UHI parameters in urban stations was conducted to examine the prevailing and critical weather conditions, as well as the associated UHI conditions in Hong Kong. Multiple Linear Regression (MLR) was used to estimate the daily maximum UHI intensity (UHI_{max}) based on a set of meteorological elements including cloud amount, wind speed, wind direction, relative humidity, and air temperature, as well as a UHI parameter of the daily maximum UHI intensity of the previous day ($UHI_{pre-max}$). The results showed that MLR-based models can explain 33% and 56% variations of the UHI_{max} in the summer and the whole year, respectively. The relative importance of each meteorological element on UHI development differed in the summer and annual periods, and the UHI_{max} tended to be intensified under high temperature conditions in the summer.

Keywords: urban heat island; subtropical climate; meteorological elements; frequency distribution; multiple linear regression



Citation: Zheng, Y.; Li, W.; Fang, C.; Feng, B.; Zhong, Q.; Zhang, D. Investigating the Impact of Weather Conditions on Urban Heat Island Development in the Subtropical City of Hong Kong. *Atmosphere* **2023**, *14*, 257. <https://doi.org/10.3390/atmos14020257>

Academic Editor: Matthew Eastin

Received: 14 December 2022

Revised: 12 January 2023

Accepted: 26 January 2023

Published: 28 January 2023



Copyright: © 2023 by the authors. Licensee MDPI, Basel, Switzerland. This article is an open access article distributed under the terms and conditions of the Creative Commons Attribution (CC BY) license (<https://creativecommons.org/licenses/by/4.0/>).

1. Introduction

The process of urbanization has gradually changed land surface properties and human activities, which has induced temperature elevation in urban areas and caused the urban heat island (UHI) phenomena [1–3]. Under the combined influence of local UHI and global warming, tropical and subtropical cities are facing higher heat-related risks in ecosystem stability, population health, and energy demand if without adaptation [4,5]. Hong Kong is one of the most densely populated and densely built subtropical cities in the world, with high exposure and vulnerability to UHI conditions [6,7]. Considerable UHI intensity and significant intraurban UHI variation have been observed in Hong Kong, due to its subtropical monsoon climate, heterogeneous built environment, and hilly mountainous geography conditions [8,9]. Previous studies in Hong Kong have investigated the spatial characteristics of UHI development through in situ UHI observations [10–12] and remote sensing techniques [13,14], most of which were performed under a clear sky and weak wind weather conditions. However, UHI variations under prevailing summer weather conditions, i.e., partly cloudy with calm winds, have received less attention [15,16].

As clouds and wind are surrogate variables related to radiative and turbulent transfer in producing air temperature change, a decrease in cloud amount and wind speed

would contribute to the local UHI development [17,18]. To classify weather conditions for UHI evolution, Oke [19] proposed a weather factor algorithm as a weather filtering tool which takes the cloud amount, cloud type, and wind speed into account [20]. Previous studies have applied cloud amount and wind speed to classify the weather conditions for UHI observation in different climate regions with varied urban built environments and geographical conditions [21,22]. One criticism of the worldwide application of the cloud–wind-based weather classification mechanism is that a high variance of UHI intensity may be observed in the prevailing weather classes, especially for cities with meteorological data highly concentrated in the specific cloud and wind ranges. Thus, examinations of a more comprehensive set of meteorological data are necessary to identify the key meteorological elements on UHI development under prevailing weather conditions.

Besides cloud and wind, recent studies have incorporated more meteorological elements and UHI indicators, such as air temperature, relative humidity, and mean sea level pressure, as well as the daily maximum UHI intensity of the previous day ($\text{UHI}_{\text{pre-max}}$), into UHI evaluation [23–25]. Moreover, Kim and Baik [26,27] have pointed out that the relative importance of multiple meteorological elements for UHI development may vary across cities and seasons. Thus, it is necessary to further examine the connection between weather conditions and UHI evolution under local urban scenarios of different cities in different climate regions for better weather control of UHI observations and analysis.

In response to the need for a better understanding of the influence of weather conditions on UHI development in Hong Kong, this study aims to characterize the frequency distribution pattern of weather conditions, investigate the impacts of multiple meteorological elements on UHI evolution, and develop weather-based UHI estimation models in summer and the whole year. First, the occurrence frequency of the UHI parameters of the daily maximum UHI intensity (UHI_{max}), the daily maximum UHI intensity of the previous day ($\text{UHI}_{\text{pre-max}}$), as well as multiple meteorological elements of cloud amount, wind speed, wind direction, relative humidity, and air temperature were examined in summer and the annual period to quantify the prevailing weather conditions in Hong Kong. Second, the frequency distribution of the UHI_{max} as a function of each meteorological element was plotted to visualize the frequency pattern of meteorological elements and their influences on UHI development. Finally, Multiple Linear Regression (MLR) was employed to establish weather-based estimation models of the UHI_{max} in Hong Kong.

2. Method

2.1. Context

Hong Kong lies on the southeast coast of China ($22^{\circ}16'50$ N, $114^{\circ}10'20$ E), with a total area of about 1104 square kilometers covering Hong Kong Island, Kowloon, and the New Territories and Islands. The terrain of Hong Kong is hilly and mountainous with steep slopes, and the elevation ranges from sea level to over 900 m above sea level [28]. Hong Kong has a monsoon-influenced subtropical climate along with seasonal variation in temperature, precipitation, humidity, and wind direction. The wind environment in Hong Kong is greatly influenced by monsoon circulation and its hilly coastal topography. Annual prevailing winds come from the east, while during the summer, the influence of southwest air streams is also significant [29].

2.2. Data

The Hong Kong Observatory operates a network of automatic weather stations located in various districts of Hong Kong to meet the increasing need for local climatic data. The Hong Kong Observatory Headquarters station (HKOH) is the longest enabled weather station located in the central urban area of Kowloon Peninsula, surrounded by compact high-rise buildings. It has been widely recognized as the representative urban station in previous climatic studies [30–32]. The Kseung Kwan O station (JKB), Shatin station (SHA), and Tun Mun station (TUN) located in the central areas of different districts of Hong Kong were also selected as urban stations to examine UHI conditions. The determination of rural

references for UHI studies is difficult for Hong Kong because local climatic conditions vary across different rural areas owing to the geographical diversity. Stations located near the coast such as Cheung Chau station and Waglan Island station have been excluded from consideration, as the recorded daily temperature profiles could be significantly influenced by the seawater temperature [33]. Ta Kwu Ling (TKL) and Lau Fu Shan (LFS) stations have been widely acknowledged as rural stations of Hong Kong [32,34,35]. The TKL station is in the northeastern rural area with a small population and lush vegetation. The LFS station is controversial due to its surrounding low-rise neighborhoods and proximity to high-rise residential developments in Tin Shui Wai. Some early studies classified LFS as a rural station [36,37], while recent studies recognized it as an urban or suburban station [32]. The study by Wu, Leung [38] found that the LFS station experienced similar diurnal temperature profiles with the urban stations located in new towns of Hong Kong. Based on the above consideration, the TKL station is designated as the representative rural station in this study. The distance between the TKL station and HKOH is around 25 km, which agrees with the distance requirement of urban and rural stations proposed by Karl, Diaz [39]. Wind records by urban or rural stations are highly modified by local geography and land cover conditions, which may deviate significantly from the background wind conditions [40]. Hence, the Waglan Island (WGL) station, which is located on Waglan Island surrounded by the sea, was designated as the representative station of background wind conditions. Geolocations and general descriptions of weather stations are presented in Figure 1 and Table 1.

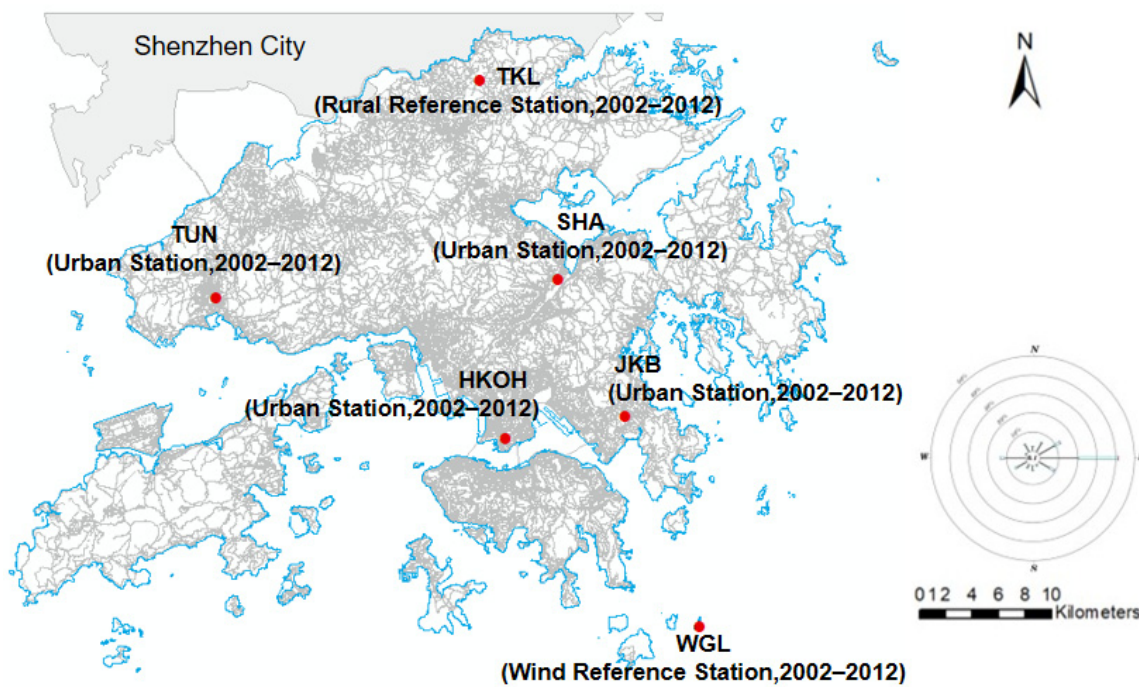


Figure 1. Location and data period of study weather conditions.

Table 1. Description of weather stations.

Station	Type	Meteorological Elements for Analysis
HKOH	Urban Representative Station	Air temperature, relative humidity, wind speed, cloud amount
JKB, SHA, TUN	Urban Station	Air temperature, relative humidity, wind speed
TKL	Rural Reference Station	Air temperature
WGL	Wind Reference Station	Wind direction

Meteorological data from HKOH, JKB, SHA, TUN, CPH, TKL station and WGL station from 2002 to 2012 at hourly intervals (a total of 96,384 h of records of 4016 days) were collected from the Hong Kong Observatory. Hong Kong has summer months from May to September [41,42]. The early May and late September periods are near the seasonal alteration with spring and autumn. Hence, data from the hot period of mid-May to mid-September (a total of 32,736 h of records of 1364 days) were included in the summer analysis.

2.3. Quantifying UHI Intensity and Daily Weather Conditions

The UHI intensity (UHII) is defined as the temperature differences between the urban and rural stations based on Equation (1):

$$\text{UHII} = T_{\text{urban}} - T_{\text{rural}} \quad (1)$$

The daily maximum UHI intensity (UHI_{max}) and daily mean UHI intensity (UHI_{mean}) are defined as the daily maximum and mean temperature difference between urban and rural stations in a diurnal cycle, respectively. The UHI_{max} and UHI_{mean} reveal the magnitude of urban warming under the influence of urbanization. A previous study by Zheng [43] found positive correlations between the $\text{UHI}_{\text{max}}/\text{UHI}_{\text{mean}}$ and daily maximum/minimum air temperature, which implies that the UHI magnitudes tend to be stronger in hot summer days. The UHI_{max} shows stronger associations with daily air temperature conditions than the UHI_{mean} . Therefore, the UHI_{max} was examined in this study as the representative parameter of UHI magnitude.

The UHI_{max} was computed as the mean values of the daily maximum UHI intensity of the four urban stations of HKOH, JKB, SHA, and TUN. The daily mean value of multiple meteorological elements were also calculated based on the records of the four urban stations, including the daily mean air temperature (Air Temp.), daily mean wind speed (Wind SPD), and daily mean relative humidity (RH). The daily mean cloud amount (CLD) was calculated based on the HKOH observation records. The daily prevailing wind direction (Wind DIR) was analyzed based on the meteorological data of the WGL station in eight directions (north, northeast, east, southeast, south, southwest, west, and northwest). The direction with the highest frequency was determined as the wind direction of the day.

2.4. Statistical Analysis

An Analysis of Variance (ANOVA) and Student's t test were applied to examine the statistical difference in the UHI conditions in the four urban stations. A distribution analysis was then conducted to examine the distribution pattern of the UHI variables and meteorological elements as the basis for multivariate analysis, while a partial correlation analysis [44] was further employed to assess the correlation between each of the two variables with the effects of the other variables removed.

Based on the results of the above analysis, multivariate analysis methods of Multiple Linear Regression (MLR) were performed to predict the UHI intensity from multiple meteorological elements. The MLR method is a widely used statistical empirical modeling method with advantages in the linear expression of the correlation between the output and input variables. However, it may yield unreliable results in the presence of collinearity between independent variables. Hence, regression diagnostics of the variance inflation factor (VIF) was incorporated to choose the final model. As a high VIF value indicates the significant collinearity of input variables, the VIF value of independent variables needs to be controlled within 2 [45].

3. Result and Analysis

3.1. ANOVA, Distribution, and Partial Correlation Analysis

A distribution analysis was performed to examine the normality of the UHI_{max} in the urban stations of HKOH, JKB, SHA, and TUN in the summer period and the whole year, and the results showed that the UHI_{max} in the four urban stations were all non-normally distributed. Thus, the data were transformed into a normal distribution through the fitted

quantile function. A one-way ANOVA was then conducted to examine the difference in the transformed normal distribution value of the UHI_{max} of the four urban stations (Table 2). Grouping information was calculated using Students’s *t* test, and the mean values of the UHI_{max} that did not share the same letter of grouping were significantly different [46]. The results showed statistically significant differences in the UHI_{max} among the urban stations both in summer and the whole year, which indicated that the UHI conditions varied across different urban areas due to the heterogeneous urban built environment and geographical conditions in Hong Kong.

Table 2. Statistics of UHI_{max} observed at four urban stations in summer and the whole year using the one-way ANOVA test (2002–2012, incomplete observations were excluded, and *n* corresponds to the number of daily observations during the study period).

Weather Station	Grouping	UHI_{max} (Summer, 2002–2012)							
		<i>n</i>	Mean	StdDev	Minimum	25%	Median	75%	Maximum
HKOH	A	1356	2.63	1.10	0.2	1.8	2.6	3.3	8.5
JKB	B	1356	1.70	1.11	−0.5	0.9	1.5	2.3	8.2
SHA	B	1354	2.22	0.92	−0.1	1.6	2.1	2.8	7.9
TUN	C	1350	2.71	1.04	−0.3	2	2.6	3.3	9.1
Weather Station	Grouping	UHI_{max} (Annual, 2002–2012)							
		<i>n</i>	Mean	StdDev	Minimum	25%	Median	75%	Maximum
HKOH	A	4008	3.01	1.74	−0.1	1.8	2.7	3.8	11
JKB	B	4005	1.91	1.53	−1.1	0.8	1.6	2.6	9.4
SHA	C	4006	2.25	1.24	−0.2	1.4	2	2.8	10
TUN	D	3999	2.77	1.41	−0.3	1.8	2.5	3.4	10.3

Averaged values of the UHI_{max} , $UHI_{pre-max}$, Wind SPD, RH, and Air Temp. of the four stations of HKOH, JKB, SHA, and TUN were further examined using a frequency analysis. As Figures 2 and 3 show, the meteorological elements of CLD, RH, and Air Temp. were negatively skewed, while Wind SPD as well as the UHI parameters of the UHI_{max} and $UHI_{pre-max}$ were positively skewed both in the summer and the whole year. In the summer, the UHI_{max} mainly ranged from 1.625 K (25% quantile) to 2.85 K (75% quantile); the CLD was highly concentrated in the range of 4.74 Octas to 6.96 Octas; the Prevailing Wind SPD ranged from 1.77 m/s to 2.62 m/s; RH was mainly distributed in the range of 75.9% to 85.2%; and Air Temp. mainly ranged from 27.13 K to 29.41 K. In the whole year, the UHI_{max} demonstrated a wider range than that in the summer, with the corresponding 25% and 75% quantile values of 1.53 K and 3.05 K. The cloud conditions in the whole year were similar to that in summer, with 50% of the records distributed in the range of 4.26 Octas to 6.96 Octas. Similar wind speed conditions were also observed in the annual period, mainly spanning from 1.80 m/s to 2.60 m/s. The major range of the RH was 71.6% to 83.8% in the whole year, while the Air Temp. ranged from 19.11 K to 27.74 K.

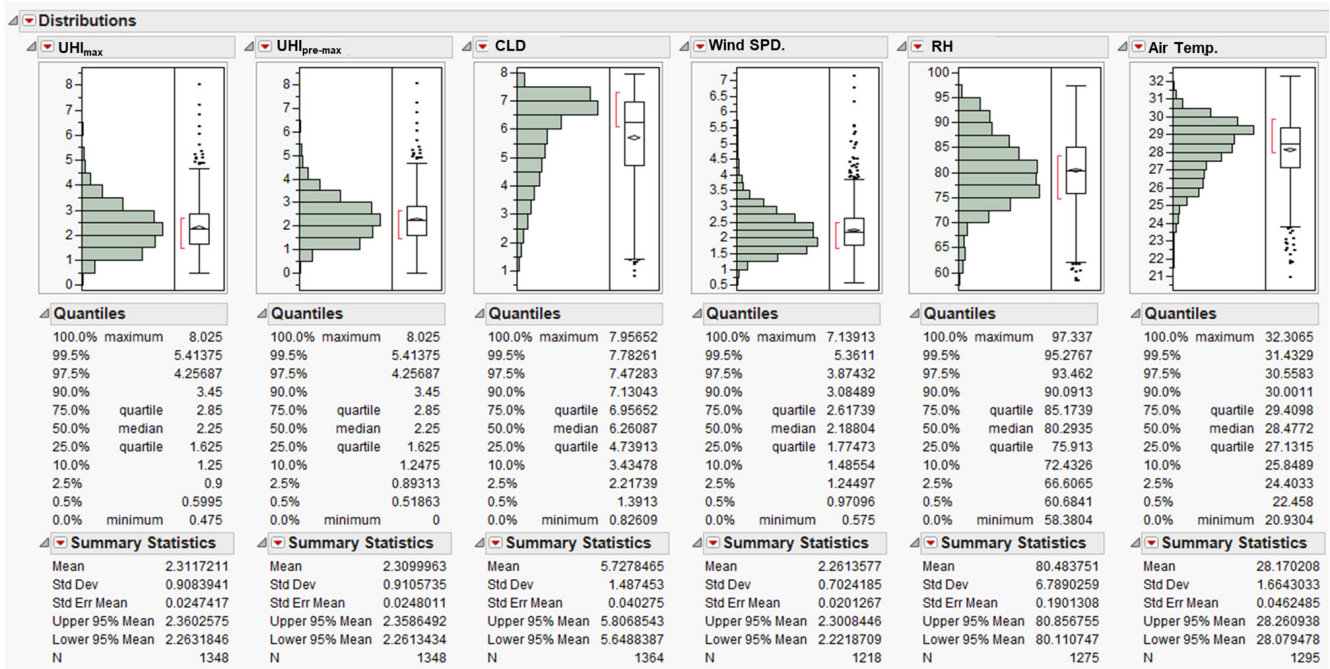


Figure 2. Distribution analysis and summary statistics of meteorological elements and UHI indicators in summer (mean values of four urban stations of HKOH, JKB, SHA, and TUN, summer, 2002–2012. *n* corresponds to the number of daily observations during the study period, and incomplete observations were excluded).

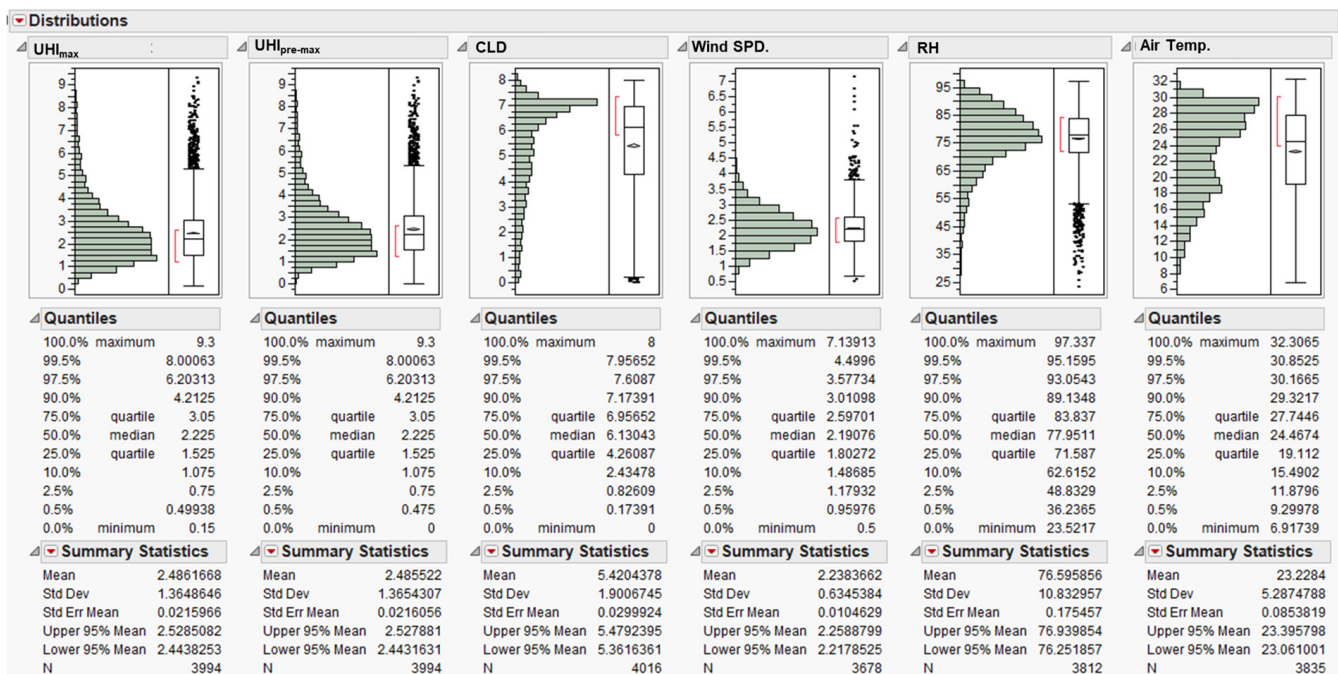


Figure 3. Distribution analysis and summary statistics of meteorological elements and UHI indicators in the whole year (mean values of four urban stations of HKOH, JKB, SHA, and TUN, summer, 2002–2012. *n* corresponds to the number of daily observations during the study period, and incomplete observations were excluded).

Tables 3 and 4 show the partial correlation coefficients of each of the two variables (UHI parameters and meteorological elements) in summer and the whole year. The partial correlation coefficients differed in the summer and the whole year. In the summer, the $UHI_{pre-max}$ and Air Temp. were positively related to the UHI_{max} , while the Wind SPD and RH were negatively related to the UHI_{max} . The CLD showed a weak correlation with UHI_{max} with a Partial R value of -0.02 . In the whole year, the $UHI_{pre-max}$ had the highest Partial R value (Partial R = 0.45) followed by the CLD (Partial R = -0.29), Wind SPD (Partial R = -0.23), and RH (Partial R = -0.23). The Partial R value between Air Temp. and UHI_{max} was -0.04 in the whole year.

Table 3. Partial correlation analysis of UHI parameters and meteorological elements (summer, 2002–2012, incomplete observations were excluded).

	UHI_{max}	$UHI_{pre-max}$	CLD	Wind SPD	RH	Air Temp.
UHI_{max}		0.32	-0.02	-0.18	-0.14	0.24
$UHI_{pre-max}$ MAX	0.32		0.05	-0.04	-0.04	0.14
CLD	-0.02	0.05		0.27	0.50	-0.22
Wind SPD.	-0.18	-0.04	0.27		-0.23	0.15
RH	-0.14	-0.04	0.50	-0.23		-0.29
Air Temp.	0.24	0.14	-0.22	0.15	-0.29	

Table 4. Partial correlation analysis of UHI parameters and meteorological elements (annual, 2002–2012, incomplete observations were excluded).

	UHI_{max}	$UHI_{pre-max}$	CLD	Wind SPD	RH	Air Temp.
UHI_{max}		0.45	-0.29	-0.23	-0.23	-0.04
$UHI_{pre-max}$	0.45		-0.03	0.03	-0.10	-0.06
CLD	-0.29	-0.03		0.22	0.47	-0.21
Wind SPD	-0.23	0.03	0.22		-0.35	0.10
RH	-0.23	-0.10	0.47	-0.35		0.30
Air Temp.	-0.04	-0.06	-0.21	0.10	0.30	

3.2. Impact of Weather Conditions and Previous-Day UHI Level on UHI Development

To further investigate the influence of multiple meteorological elements and the previous-day UHI condition on UHI development, the frequency distribution of the UHI_{max} as a function of the CLD, Wind SPD, Wind DIR, RH, and Air Temp., as well as the $UHI_{pre-max}$, were examined. Figure 4 shows that a small amount of the summer data fell in the range with a cloud amount below 2 Oktas (clear sky condition), and the associated UHI_{max} was most concentrated in the range of 2 K to 4 K. In comparison, partly cloudy conditions (2–7 Octas) demonstrated a wider range of the UHI_{max} from 0 K to 9 K. A high UHI_{max} above 6 K in the summer was observed in partly cloudy conditions from 3 Oktas to 6 Oktas, which implies significant heat risks under the prevailing partly cloudy days in the summer in Hong Kong. Figure 4b shows that clear sky conditions occurred with a higher frequency in the whole year than in the summer. The highest level of the UHI_{max} for the whole year appeared under clear sky conditions with the peak value around 10 K, and a high UHI_{max} level above 6 K also mainly occurred under clear sky conditions.

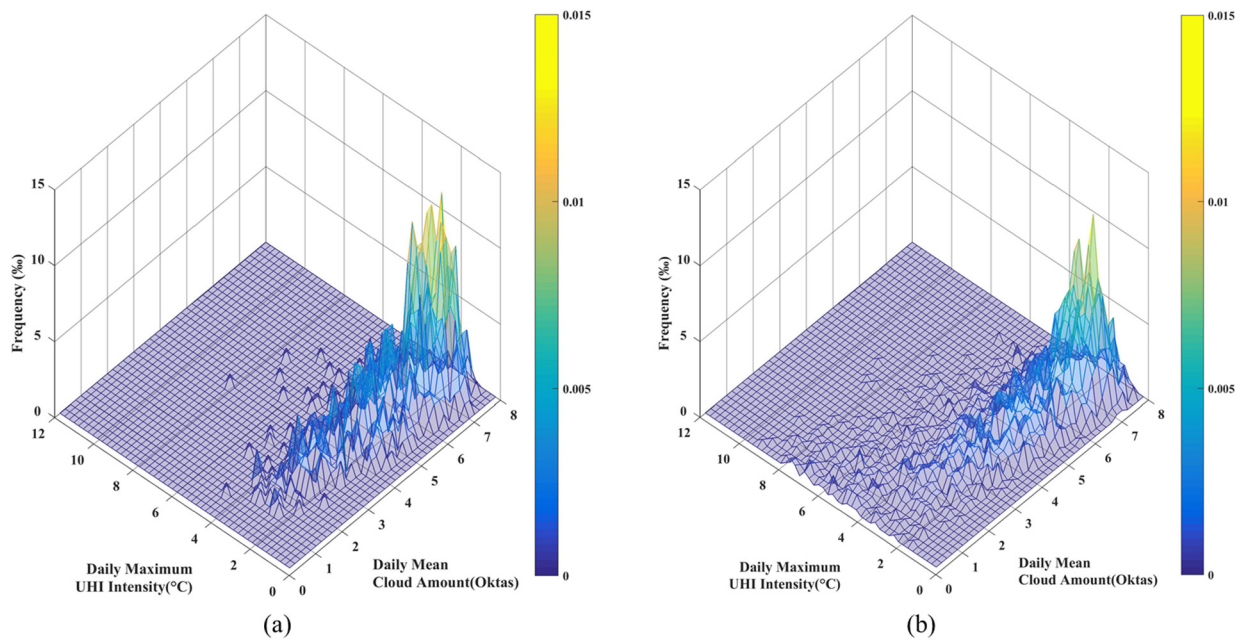


Figure 4. Frequency distribution of UHI_{max} as a function of cloud amount (2002–2012, (a) summer, (b) annual).

Figure 5 demonstrates that the Wind SPD in Hong Kong mainly ranged from 1.5 m/s to 3 m/s both in the summer and the whole year. The UHI_{max} in high wind speed conditions above 6 m/s was limited to 3 K in the summer and the whole year. As seen in Figure 5a, the UHI_{max} in light wind conditions (under 3 m/s) in the summer mainly varied in the range of 2 K to 6 K. A high UHI_{max} spanning from 6 K to 8 K in the summer was generally associated with light wind speeds around 2 m/s. Figure 5b shows that, in the whole year period, the occurrence frequency of a high UHI_{max} above 6 K was higher than that in the summer, which was generally associated with light wind conditions with a Wind SPD under 3 m/s.

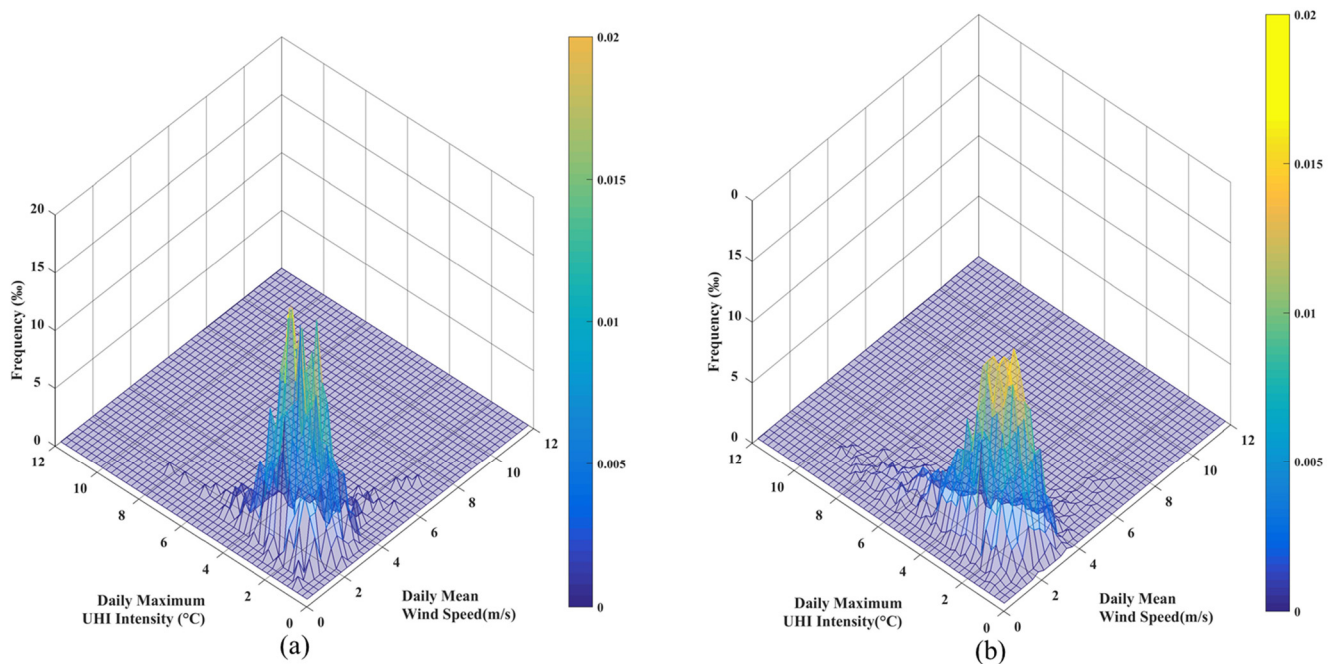


Figure 5. Frequency distribution of UHI_{max} as a function of wind speed (2002–2012, (a) summer, (b) annual).

As shown in Figure 6, the prevailing wind directions varied in the summer and the whole year period. Summertime prevailing winds in Hong Kong come from the east and southwest, while the annual prevailing wind directions come from the east. Figure 6a shows that, in the summertime prevailing winds from the east and southwest, the UHI_{max} mainly ranged from 2 K to 4 K. A high UHI_{max} above 6 K mainly occurred with winds from the west and southwest. As can be seen in Figure 6b, the annual prevailing east and northeast wind conditions experienced the broadest range of the UHI_{max} with peaks and troughs around 10 K and near 0 K, respectively. A high UHI_{max} above 6 K was mainly distributed in the north, northeast, east, and west categories.

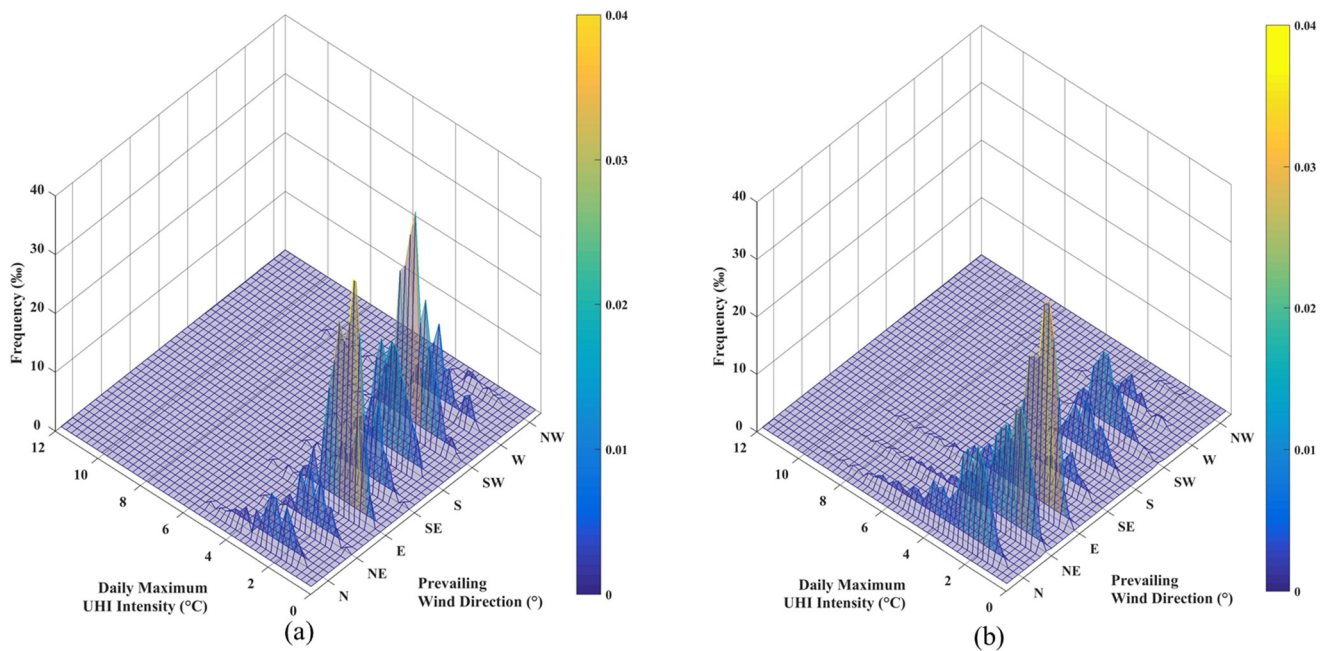


Figure 6. Frequency distribution of UHI_{max} as a function of wind direction (2002–2012, (a) summer, (b) annual).

Figure 7 demonstrates that the UHI_{max} was positively correlated with the $\text{UHI}_{\text{pre-max}}$, which was influenced by the weather conditions of the previous day. The frequency distribution pattern of the $\text{UHI}_{\text{pre-max}}$ was consistent with that of the UHI_{max} , which mainly fell in the range of 2 K to 4 K both in the summer and the whole year. Most of the differences between the UHI_{max} and $\text{UHI}_{\text{pre-max}}$ were within 2 K. As Figure 7a shows, a UHI_{max} above 6 K in summer was associated with the $\text{UHI}_{\text{pre-max}}$ of 2 K to 4 K, which implies the low occurrence probability of continuous high UHI_{max} conditions. Figure 7b demonstrates that a UHI_{max} above 6 K in the whole year has a wider range of the $\text{UHI}_{\text{pre-max}}$ compared to that in summer, with the corresponding $\text{UHI}_{\text{pre-max}}$ values spanning from 2 K to 8 K. The results indicate the high probability of consecutive high UHI_{max} conditions in the whole year period.

Hong Kong experiences humid weather both in the summer and the whole year (Figure 8). Figure 8a shows that the RH in the summer was highly concentrated in the high RH range of 70% to 100%, and the corresponding UHI_{max} had a wide range of 0 K to 8 K. A high UHI_{max} above 6 K is associated with an RH value ranging from 70% to 80%. As Figure 8b shows, the UHI_{max} tended to increase as RH decreased. A high UHI_{max} above 6 K in the whole year was distributed in the wider RH range of 20% to 90% compared to that in summer, and a UHI_{max} higher than 8 K was generally associated with a comparatively lower RH range of 40% to 60%.

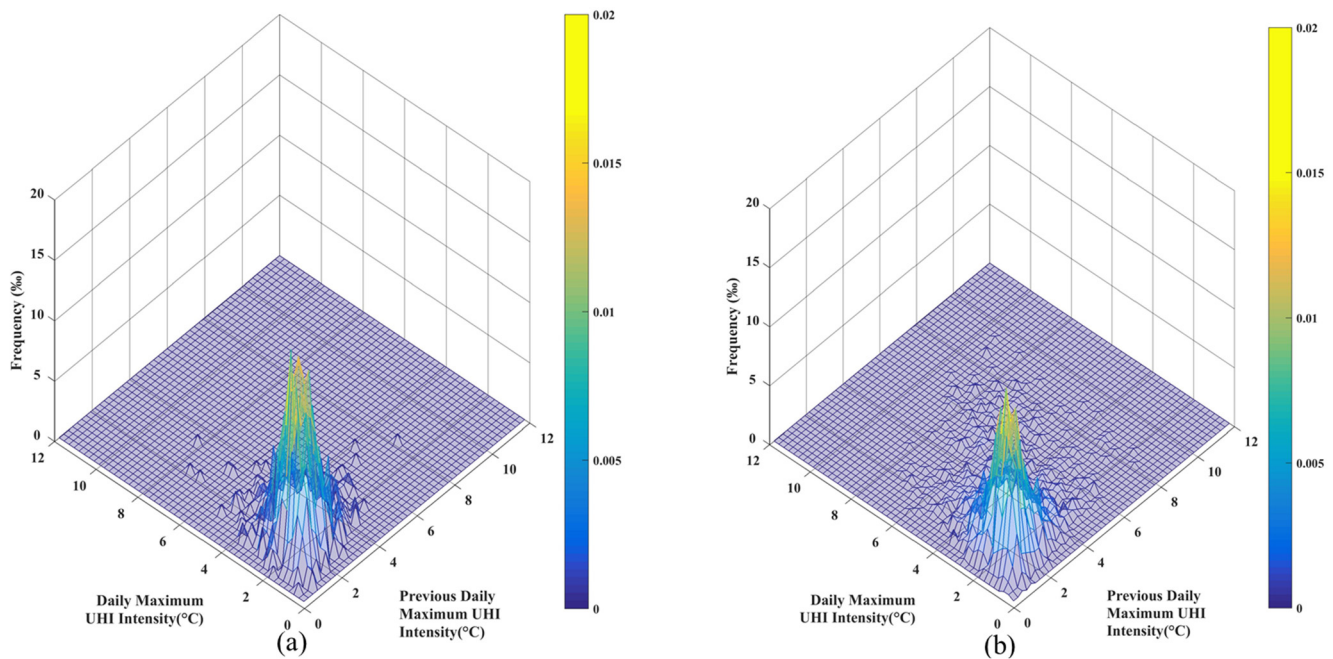


Figure 7. Frequency distribution of UHI_{max} as a function of the previous-day UHI_{max} (2002–2012, (a) summer, (b) annual).

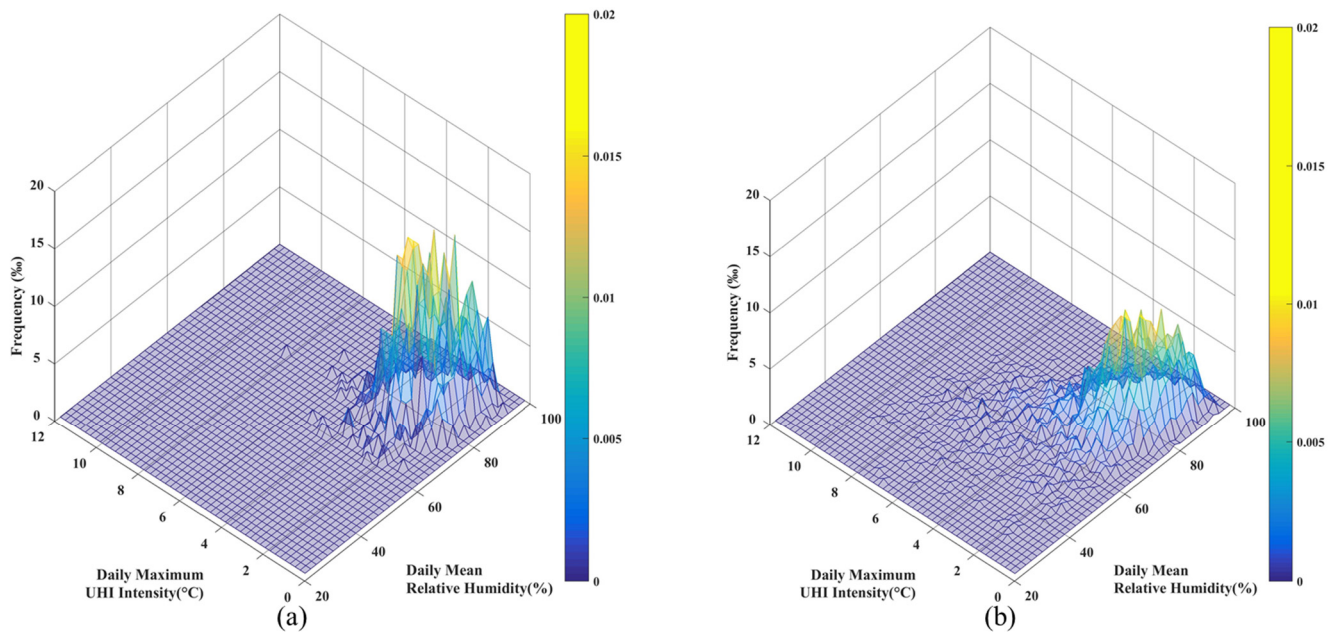


Figure 8. Frequency distribution of UHI_{max} as a function of relative humidity (2002–2012, (a) summer, (b) annual).

Regarding the correlation between the UHI_{max} and air temperature, different patterns were observed in the annual and summer periods. Figure 9a shows that hot summer days tended to experience a higher UHI_{max}, and a UHI_{max} above 6 K usually took place with a daily mean air temperature over 27 K. From an annual perspective, the UHI_{max} was highly concentrated in the range of 2 K to 4 K in the summertime with an air temperature above 25 K, while in other seasons with an air temperature below 25 K, the UHI_{max} was more equally distributed in the range of 1 K to 4 K (Figure 9b).

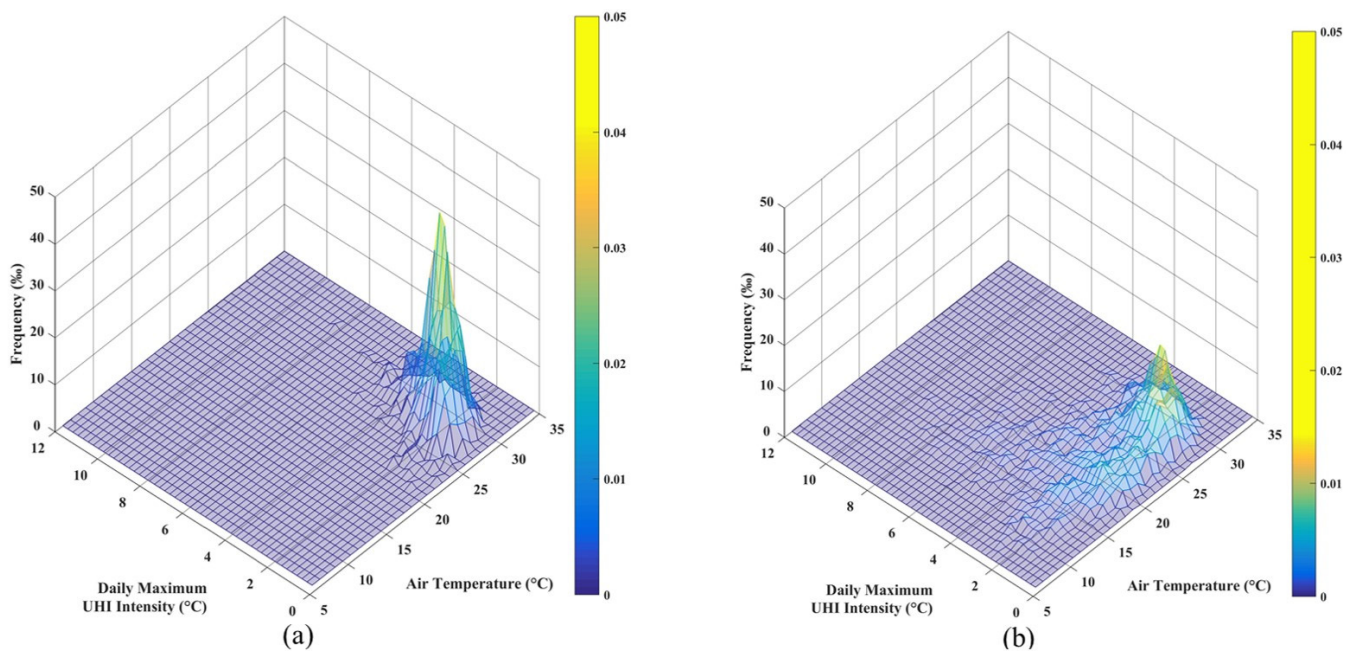


Figure 9. Frequency distribution of UHI_{max} as a function of air temperature (2002–2012, (a) summer, (b) annual).

3.3. Modeling Daily Maximum UHI Intensity Based on Meteorological Elements and Previous UHI Conditions Using MLR

A Multiple Linear Regression (MLR) was performed to establish weather-based UHI_{max} estimation models in the summer and the whole year. The UHI_{pre-max}, CLD, Wind SPD, Air Temp., and RH were put into the stepwise MLR analysis as independent variables, and incomplete observations were excluded from the analysis. VIF values were calculated to avoid the inflation of the regression model due to the lack of independence between the input variables. Forward stepwise selection methods were used to develop the UHI_{max} models (Tables 5 and 6). For the MLR analysis, we selected input parameters following the stopping rule of the minimum Akaike information criterion (AIC), and the automatic parameter selection order was basically consistent with the partial correlation analysis. The two models were validated by a 10-fold cross validation method, and the corresponding R² values were at a similar level with an adjusted R². The VIF values of the predictors were not higher than two, which means that no significant multicollinearity existed between the predictors.

Table 5. Statistical model of UHI_{max} in summer using stepwise MLR (2002–2012, incomplete observations were excluded, * statistically significant).

Forward Stepwise MLR					
Step	Parameter	Action	R ²	10-Fold Cross Validation R ²	AICc
1	Air Temp.	Entered	0.20	0.20	2817.3
2	UHI _{pre-max}	Entered	0.28	0.28	2686.7
3	Wind SPD	Entered	0.31	0.30	2649.5
4	RH	Entered	0.33	0.32	2615.4
5	Best Model	Specific	0.33	0.32	2615.4

Table 5. Cont.

Summary of Fit							
Dependent Variable	R ²	Adjusted R ²	RMSE	Mean of Response	p Value	Observations	10-Fold Cross Validation R ²
Daily Maximum UHI Intensity (UHI _{max})	0.33	0.33	0.74	2.33	<0.0001 *	1170	0.32
Parameter Estimates							
Term	Estimate	Std Error	t Ratio	Prob > t	VIF		
Intercept	−0.10	0.67	−0.15	0.8807	-		
Air Temp.	0.14	0.02	9.12	<0.0001 *	1.53		
UHI _{pre-max}	0.29	0.03	11.18	<0.0001 *	1.12		
Wind SPD	−0.21	0.03	−6.83	<0.0001 *	1.01		
RH	−0.02	0.004	−6.04	<0.0001 *	1.46		

$$UHI_{max} = -0.10 + 0.14 \times \text{Air Temp.} + 0.29 \times UHI_{pre-max} - 0.21 \times \text{Wind SPD} - 0.02 \times \text{RH} \quad (2)$$

Table 6. Statistical model of UHI_{max} of the whole year using stepwise MLR (2002–2012, incomplete observations were excluded, * statistically significant).

Forward Stepwise MLR							
Step	Parameter	Action	R ²	10-Fold Cross Validation R ²	AICc		
1	UHI _{pre-max}	Entered	0.37	0.37	10,717.6		
2	CLD	Entered	0.51	0.51	9821.0		
3	RH	Entered	0.53	0.53	9692.0		
4	Wind SPD	Entered	0.56	0.55	9485.6		
5	Air Temp.	Entered	0.56	0.55	9481.6		
6	Best Model	Specific	0.56	0.55	9481.6		
Summary of Fit							
Dependent Variable	R ²	Adjusted R ²	RMSE	Mean of Response	p value	Observations	10-fold Cross Validation R ²
UHI _{max}	0.56	0.56	0.91	2.50	<0.0001 *	3578	0.55
Parameter Estimates							
Term	Estimate	Std Error	t Ratio	Prob > t	VIF		
Intercept	5.74	0.17	34.75	<0.0001 *	-		
UHI _{pre-max}	0.38	0.01	29.86	<0.0001 *	1.31		
CLD	−0.19	0.01	−17.84	<0.0001 *	1.85		
RH	−0.03	0.002	−14.17	<0.0001 *	2.00		
Wind SPD	−0.37	0.03	−14.29	<0.0001 *	1.15		
Air Temp.	−0.008	0.003	−2.45	<0.0001 *	1.14		

$$UHI_{max} = 5.74 + 0.38 \times UHI_{pre-max} - 0.19 \times \text{CLD} - 0.03 \times \text{RH} - 0.37 \times \text{Wind SPD} - 0.008 \times \text{Air Temp.} \quad (3)$$

The selected predictors of the UHI_{max} in the summer included Air Temp., UHI_{pre-max}, SPD, and RH (Table 5). The stepwise parameter selection in the summer showed that Air Temp. could explain around 20% of the UHI_{max} variation independently. A combination of

Air Temp. and $\text{UHI}_{\text{pre-max}}$ accounted for 28% of the UHI_{max} variation. The combination of the four selected predictors (Air Temp., $\text{UHI}_{\text{pre-max}}$, Wind SPD, and RH) showed around 6% improvement in the fitting performance. In summary, the MLR model could explain around 33% of the UHI_{max} variation in the summer, and the root mean square error was 0.74. It indicates that every 1 K increase in air temperature, 1 K increase in the $\text{UHI}_{\text{pre-max}}$, 1 m/s decrease in the wind speed, or 10% decrease in the relative humidity was associated with a rise in the UHI_{max} of 0.14 K, 0.29 K, 0.21 K, and 0.2 K, respectively.

The annual MLR analysis results showed that the strongest predictor of the UHI_{max} was the $\text{UHI}_{\text{pre-max}}$, followed by the CLD and RH (Table 6). A total of five predictors ($\text{UHI}_{\text{pre-max}}$, CLD, RH, Wind SPD, and Air Temp.) explained around 56% of the annual UHI_{max} variation, and the root mean square error was 0.91. In the annual MLR model, for every 1 K increase in the $\text{UHI}_{\text{pre-max}}$, 1 Octas decrease in the cloud amount, 10% decrease in the relative humidity, 1 m/s decrease in the wind speed, or 1 K decrease in the air temperature, the corresponding UHI_{max} elevation was 0.38 K, 0.19 K, 0.3 K, 0.37 K, and 0.008 K, respectively.

4. Discussion

The results of partial correlation analysis and MLR analysis indicated that the significance and magnitude of influence of meteorological elements/ $\text{UHI}_{\text{pre-max}}$ on the UHI_{max} in Hong Kong differed between the summer and the annual periods. In the summer, the Air Temp., $\text{UHI}_{\text{pre-max}}$, Wind SPD, and RH were key predictors of the UHI_{max} selected by the stepwise MLR model. In the whole year, the $\text{UHI}_{\text{pre-max}}$, CLD, RH, Wind SPD, and Air Temp. were key predictors. Impacts of meteorological elements on UHI development are further discussed as follows:

4.1. Cloud Amount

As the distribution analysis results showed, the dominant sky type in Hong Kong was partly cloudy (3–7 Oktas) both in the summer and the whole year. According to the 3D plot analysis and partial correlation analysis, the cloud amount had a negative influence on UHI development. As clouds scatter and absorb short-wave radiation, the amount of short-wave radiation is reduced from reaching the land surface. Clouds also serve as an isolation layer to absorb and re-emit the long-wave heat release from the land surface, so the radiative cooling process both in urban and rural areas is restricted and the associated temperature difference is also limited. Therefore, the UHI intensity decreases when the cloud amount increases.

4.2. Wind Speed

The average wind speed in the four stations of HKOH, JKB, SHA, and TUN was most concentrated in the range of 1.7 m/s to 2.6 m/s both in the summer and the whole year. Due to the high-density urban built environment, urban areas in Hong Kong generally experience weak wind conditions. As low wind speeds limit convective heat exchange, hot air would be trapped inside urban areas, which results in strengthened UHI conditions during weak wind conditions. Thus, in high-density urban areas, wind corridors need to be constructed and preserved to facilitate air ventilation for UHI mitigation. In new development areas, it is essential to optimize the configuration of buildings, open spaces, and vegetated areas to ensure effective ventilation in newly built-up areas.

4.3. Wind Direction

As can be seen from the 3D plot frequency analysis, prevailing winds in the summer come from the east, southwest, and west. A considerable UHI_{max} above 6 K was observed in west wind conditions in the summer. In the summer, Hong Kong is dominantly influenced by the southwest monsoon, and the prevailing winds veer from easterlies to southeasterlies. In the whole year, prevailing winds come from the east, northeast, north, and southwest. A UHI_{max} above 6 K generally occurs when winds come from the north, northeast, and

northwest in an annual perspective. A possible reason is that the continental airstreams from the north are generally associated with a low cloud amount and low relative humidity, which contributes to the more significant heat release of rural areas during night and accordingly enlarge the temperature difference between urban and rural areas.

4.4. $UHI_{pre-max}$

The $UHI_{pre-max}$ was positively correlated with the UHI_{max} due to the heat storage in the urban structure, which raises an alert concerning the successive occurrence of a high UHI intensity. The $UHI_{pre-max}$ can be considered an indicator of the weather conditions of the previous day. The partial correlation analysis and MLR results showed that the $UHI_{pre-max}$ was the strongest explanatory variable of the UHI_{max} in the whole year. The relative importance of the $UHI_{pre-max}$ in predicting the UHI_{max} declined in the summer in Hong Kong, which may have been due to the influence of active and unstable monsoons, thermal convection, and tropical cyclones in the summer.

4.5. Relative Humidity

Relative humidity had a negative correlation with the UHI_{max} . A higher relative humidity expresses a higher ratio of water vapor pressure to saturated water vapor pressure and accordingly limits the cooling process through evaporation. Relative humidity is a key predictor of the UHI_{max} during the summertime in Hong Kong, possibly owing to its sensitivity to the alternating synoptic conditions of subtropical high pressure, tropical depression, and maritime airflows in the summer.

4.6. Air Temperature

The annually highest level of the UHI is favored by the fine weather in winter, with a lower air temperature, lower relative humidity, lower cloud cover, and stronger monsoon wind. Thus, the MLR analysis based on the annual data suggested a negative correlation between air temperature and the UHI_{max} . Conversely, anticyclonic conditions bring fine weather with a relatively high air temperature and low relative humidity in the summer. Thus, air temperature was positively correlated with the UHI_{max} in the summer, which implies that hot summer days bring a more severe threat of an urban heat island.

5. Conclusions

In this study, meteorological archives from six weather stations of the Hong Kong Observatory, including four urban stations, one rural reference station, and one wind direction reference station, were examined to quantify the influence of meteorological elements on the daily maximum UHI intensity. This study examined the influence of weather conditions on UHI evolution in Hong Kong based on a multiple-indicator analysis that included cloud amount, wind speed, wind direction, relative humidity, air temperature, and the maximum UHI intensity of the previous day. An intuitive understanding of the relationships between meteorological elements/ $UHI_{pre-max}$ and the UHI_{max} was presented through 3D frequency plots. Statistical models of the UHI_{max} in the summer and the whole year were developed based on multiple meteorological elements and the UHI parameter of the $UHI_{pre-max}$. The main findings of this study are summarized as follows:

1. A considerable UHI intensity was recorded under the clear sky and weak wind conditions, which occurred at a low frequency both in the summer and in the whole year. Partly cloudy and light wind conditions were the dominant weather types in the summer in Hong Kong, under which the most considerable variation in the UHI_{max} was observed, and a high UHI_{max} above 6 K was documented.
2. In the summer, key predictors of the UHI_{max} were air temperature, the $UHI_{pre-max}$, wind speed, and relative humidity. The air temperature was positively correlated with the UHI_{max} , which implies that the UHI intensity tended to be intensified under the high temperature weather conditions. High-density urban areas may be exposed to a higher frequency, magnitude, and duration of extreme heat events due to the

reinforcement of the UHI effects. Wind speed is another key meteorological element influencing UHI_{\max} , and thus improving air ventilation in urban areas would benefit local UHI mitigation.

In the whole year, $\text{UHI}_{\text{pre-max}}$ was the most important predictor of the UHI_{\max} , which suggests that UHI development is influenced by the weather conditions and heat storage of urban structures of the previous day. The cloud amount is the most important meteorological element in determining the UHI_{\max} in the whole year period. Sufficient cloud thickness blocks short-wave solar radiation from reaching the ground and absorbing and reflecting the released long-wave radiation, which results in the decrease in the UHI_{\max} . Wind speed, relative humidity, and air temperature were also included in the MLR stepwise selection procedure in predicting the UHI_{\max} in the whole year. The air temperature showed a reverse influence on the UHI_{\max} in the whole year and the summer, as cooler seasons had a higher occurrence frequency of clear sky conditions, which are ideal for UHI development.

3. The MLR method showed the influence magnitude of multiple meteorological elements and the $\text{UHI}_{\text{pre-max}}$ on the UHI_{\max} , through its simple linear structure among the input and output variables. The findings suggest that, in addition to cloud amount and wind speed, air temperature, relative humidity, and the $\text{UHI}_{\text{pre-max}}$ also need to be considered to understand the influence of weather conditions on UHI development, which is helpful to better control the weather for UHI observations. As the prevailing weather conditions in Hong Kong in the summer and the whole year are with a high cloud cover of 6–7 Octas, weak wind speed of 1.5–2.5 m/s, and high relative humidity of 70–85%, it is necessary to conduct UHI observations under the prevailing high cloud cover, weak wind, and high relative humidity conditions to evaluate local UHI patterns. In the summer, high air temperature conditions are critical for UHI observations, as the UHI_{\max} is exacerbated as the air temperature rises and the high UHI conditions further exacerbate local high temperatures. Summer days with winds coming from the west are also critical for UHI observations, as it is possible to experience a high UHI_{\max} .

This study examined the daily maximum UHI conditions in Hong Kong based on HKOH weather station records through frequency analysis, partial correlation analysis, and MLR analysis. The findings will help researchers and planners obtain quantitative knowledge of the prevailing weather conditions of Hong Kong, understand the connections between meteorological elements and the daily maximum UHI intensity, and identify key parameters for the weather control of UHI observations. It uses simple and graphical presentations of climatic information through 2D and 3D frequency plots of UHI parameters and meteorological elements, which would serve as an intuitive and quantitative knowledge basis of weather control of UHI observations and spatial analysis. The refined weather control makes it possible to identify the hot spots of the UHI based on the observed data and develop urban heat mitigation and adaptation strategies for a healthier urban environment.

A limitation of this study is that only meteorological records of six weather stations (four urban stations, one rural station, and one wind reference station) were analyzed to examine the influence of weather conditions on UHI evolution. In future studies, comprehensive records from the HKOH weather station's network should be employed to assess the intraurban variability of the UHI under different weather conditions. In addition, it only focused on the analysis of the daily maximum UHI intensity, while the differentiation of the daytime and nighttime UHI intensity was not discussed. It is necessary to further analyze the daytime and nighttime UHI evolution mechanism based on the meteorological data of more weather stations and to quantify the daytime and nighttime UHI characteristics to provide reference for the weather control of UHI observations and heat risk analysis.

Author Contributions: Conceptualization, Y.Z. and D.Z.; methodology, Y.Z.; software, Y.Z. and D.Z.; validation, W.L. and C.F.; formal analysis, Y.Z.; investigation, Y.Z.; resources, Y.Z. and D.Z.; data curation, Y.Z.; writing—original draft preparation, Y.Z.; writing—review and editing, Y.Z.

and D.Z.; visualization, W.L., C.F., B.F., and Q.Z.; supervision, D.Z.; project administration, Y.Z.; funding acquisition, Y.Z. and D.Z. All authors have read and agreed to the published version of the manuscript.

Funding: This study was supported by the Guangdong Philosophy and Social Science Foundation (Grant No. GD22CGL38), the Guangzhou Science and Technology Program (Grant No. 202201020541), the Guangdong Basic and Applied Basic Research Foundation (Grant No. 2022A1515010171), the Guangzhou Philosophy and Social Science Planning 2022 Annual Project (Grant No. 2022GZQN19), the Science and Technology Program of Guangzhou University (Grant No. PT252022006), and the Opening Fund of State Key Laboratory of Green Building in Western China (Grant No. LSKF202305).

Institutional Review Board Statement: Not applicable.

Informed Consent Statement: Not applicable.

Data Availability Statement: Data sharing is not applicable to this article.

Acknowledgments: The authors wish to thank Chao Ren, Edward Ng, Kevin Lau, Yuan Shi, editors, and anonymous reviewers for valuable suggestions on this study, and Douglas Zhang for his help with the language.

Conflicts of Interest: The authors declare no conflict of interest.

References

- Oke, T.R. The Energetic Basis of the Urban Heat Island. *Q. J. R. Meteorol. Soc.* **1982**, *108*, 1–24. [\[CrossRef\]](#)
- Oke, T.R. Street design and urban canopy layer climate. *Energy Build.* **1988**, *11*, 103–113. [\[CrossRef\]](#)
- Landsberg, H.E. *The Urban Climate*; Academic Press: Cambridge, MA, USA, 1981; Volume 28.
- Hua, J.; Zhang, X.; Ren, C.; Shi, Y.; Lee, T.-C. Spatiotemporal assessment of extreme heat risk for high-density cities: A case study of Hong Kong from 2006 to 2016. *Sustain. Cities Soc.* **2021**, *64*, 102507. [\[CrossRef\]](#)
- Morakinyo, T.E.; Ren, C.; Shi, Y.; Lau, K.K.-L.; Tong, H.-W.; Choy, C.-W.; Ng, E. Estimates of the impact of extreme heat events on cooling energy demand in Hong Kong. *Renew. Energy* **2019**, *142*, 73–84. [\[CrossRef\]](#)
- Ho, H.C.; Lau, K.K.-L.; Ren, C.; Ng, E. Characterizing prolonged heat effects on mortality in a sub-tropical high-density city, Hong Kong. *Int. J. Biometeorol.* **2017**, *61*, 1935–1944. [\[CrossRef\]](#)
- Ho, J.Y.; Shi, Y.; Lau, K.K.; Ng, E.Y.; Ren, C.; Goggins, W.B. Urban heat island effect-related mortality under extreme heat and non-extreme heat scenarios: A 2010–2019 case study in Hong Kong. *Sci. Total Environ.* **2023**, *858*, 159791. [\[CrossRef\]](#)
- Shi, Y.; Ren, C.; Luo, M.; Ching, J.; Li, X.; Bilal, M.; Fang, X.; Ren, Z. Utilizing world urban database and access portal tools (WUDAPT) and machine learning to facilitate spatial estimation of heatwave patterns. *Urban Clim.* **2021**, *36*, 100797. [\[CrossRef\]](#)
- Lau, K.K.-L.; Chung, S.C.; Ren, C. Outdoor thermal comfort in different urban settings of sub-tropical high-density cities: An approach of adopting local climate zone (LCZ) classification. *Build. Environ.* **2019**, *154*, 227–238. [\[CrossRef\]](#)
- Nichol, J.; Fung, W.Y.; Lam, K.-s.; Wong, M.S. Urban heat island diagnosis using ASTER satellite images and ‘in situ’ air temperature. *Atmos. Res.* **2009**, *94*, 276–284. [\[CrossRef\]](#)
- Giridharan, R.; Ganesan, S.; Lau, S. Daytime urban heat island effect in high-rise and high-density residential developments in Hong Kong. *Energy Build.* **2004**, *36*, 525–534. [\[CrossRef\]](#)
- Giridharan, R.; Lau, S.; Ganesan, S. Nocturnal heat island effect in urban residential developments of Hong Kong. *Energy Build.* **2005**, *37*, 964–971. [\[CrossRef\]](#)
- Fung, W.Y.; Lam, K.S.; Nichol, J.; Wong, M.S. Derivation of nighttime urban air temperatures using a satellite thermal image. *J. Appl. Meteorol. Climatol.* **2009**, *48*, 863–872. [\[CrossRef\]](#)
- Nichol, J. Remote sensing of urban heat islands by day and night. *Photogramm. Eng. Remote Sens.* **2005**, *71*, 613–621. [\[CrossRef\]](#)
- Ng, E.; Cheng, V.; Gadi, A.; Mu, J.; Lee, M.; Gadi, A. Defining standard skies for Hong Kong. *Build. Environ.* **2007**, *42*, 866–876. [\[CrossRef\]](#)
- Li, H.W.; Lam, J.C. An analysis of climatic parameters and sky condition classification. *Build. Environ.* **2001**, *36*, 435–445. [\[CrossRef\]](#)
- He, B.-J. Potentials of meteorological characteristics and synoptic conditions to mitigate urban heat island effects. *Urban Clim.* **2018**, *24*, 26–33. [\[CrossRef\]](#)
- Santamouris, M.; Kolokotsa, D. *Urban Climate Mitigation Techniques*; Routledge: New York, NY, USA, 2016.
- Oke, T.R. An algorithmic scheme to estimate hourly heat island magnitude. In Proceedings of the 2nd Sym Urban Env, Albuquerque, NM, USA, 2–6 November 1998.
- Stewart, I.D. Redefining the Urban Heat Island. Ph.D. Thesis, University of British Columbia, Vancouver, BC, Canada, 2011.
- Emmanuel, R.; Krüger, E. Urban heat island and its impact on climate change resilience in a shrinking city: The case of Glasgow, UK. *Build. Environ.* **2012**, *53*, 137–149. [\[CrossRef\]](#)
- Coseo, P.; Larsen, L. How factors of land use/land cover, building configuration, and adjacent heat sources and sinks explain Urban Heat Islands in Chicago. *Landsc. Urban Plan.* **2014**, *125*, 117–129. [\[CrossRef\]](#)

23. Ganbat, G.; Han, J.-Y.; Ryu, Y.-H.; Baik, J.-J. Characteristics of the urban heat island in a high-altitude metropolitan city, Ulaanbaatar, Mongolia. *Asia-Pac. J. Atmos. Sci.* **2013**, *49*, 535–541. [[CrossRef](#)]
24. Hoffmann, P.; Krueger, O.; Schlünzen, K.H. A statistical model for the urban heat island and its application to a climate change scenario. *Int. J. Climatol.* **2012**, *32*, 1238–1248. [[CrossRef](#)]
25. Morris, C.; Simmonds, I. Associations between varying magnitudes of the urban heat island and the synoptic climatology in Melbourne, Australia. *Int. J. Climatol.* **2000**, *20*, 1931–1954. [[CrossRef](#)]
26. Kim, Y.-H.; Baik, J.-J. Maximum urban heat island intensity in Seoul. *J. Appl. Meteorol.* **2002**, *41*, 651–659. [[CrossRef](#)]
27. Kim, Y.-H.; Baik, J.-J. Daily maximum urban heat island intensity in large cities of Korea. *Theor. Appl. Climatol.* **2004**, *79*, 151–164. [[CrossRef](#)]
28. Dai, F.; Lee, C. Landslide characteristics and slope instability modeling using GIS, Lantau Island, Hong Kong. *Geomorphology* **2002**, *42*, 213–228. [[CrossRef](#)]
29. HKPD; CUHK. *Urban Climatic Map and Standards for Wind Environment—Feasibility Study, Final Report*; CUHK: Ma Liu Shui, Hong Kong, 2009.
30. Yim, W.; Ollier, C. Managing planet earth to make future development more sustainable: Climate change and Hong Kong. *Quart. Sci.* **2009**, *29*, 190–198.
31. Lam, C.Y. On climate changes brought about by urban living. Designing high-density cities for social and environmental sustainability. In *Designing High-Density Cities*; Routledge: New York, NY, USA, 2010; pp. 55–61.
32. Memon, R.A.; Leung, D.Y.; Liu, C.-H. An investigation of urban heat island intensity (UHII) as an indicator of urban heating. *Atmos. Res.* **2009**, *94*, 491–500. [[CrossRef](#)]
33. Sakakibara, Y.; Owa, K. Urban–rural temperature differences in coastal cities: Influence of rural sites. *Int. J. Climatol.* **2005**, *25*, 811–820. [[CrossRef](#)]
34. Fung, W.Y. *Characterizing Urban Heat Island and Its Effects in Hong Kong*. Ph.D. Thesis, The Hong Kong Polytechnic University, Hong Kong, China, 2010.
35. Siu, L.W.; Hart, M.A. Quantifying urban heat island intensity in Hong Kong SAR, China. *Environ. Monit. Assess.* **2013**, *185*, 4383–4398. [[CrossRef](#)]
36. Leung, Y.K. *Climate Change in Hong Kong*. *Hong Kong Meteorological Society Bulletin*; Hong Kong Observatory: Hong Kong, China, 2004.
37. Leung, Y.K.; Ng, T.S. *Regional Temperature Variation in Winter of Hong Kong*; Hong Kong Observatory: Hong Kong, China, 1997.
38. Wu, M.C.; Leung, Y.; Lui, W.; Lee, T. A study on the difference between urban and rural climate in Hong Kong. *Meteorol.* **2009**, *35*, 71–79.
39. Karl, T.R.; Diaz, H.F.; Kukla, G. Urbanization: Its detection and effect in the United States climate record. *J. Clim.* **1988**, *1*, 1099–1123. [[CrossRef](#)]
40. HKPD; CUHK. *Urban Climatic Map and Standards for Wind Environment—Feasibility Study: Technical Digest*; Chinese University of Hong Kong: Hong Kong, China, 2009.
41. Corlett, R.T. Characteristics of vertebrate-dispersed fruits in Hong Kong. *J. Trop. Ecol.* **1996**, *12*, 819–833. [[CrossRef](#)]
42. Yan, Y.Y. Climate and residential electricity consumption in Hong Kong. *Energy* **1998**, *23*, 17–20. [[CrossRef](#)]
43. Zheng, Y. *Planning Strategies for Urban Heat Island Mitigation: An Application of Local Climate Zone into the High-Density City of Hong Kong*. Ph.D. Thesis, The Chinese University of Hong Kong, Hong Kong, China, 2016.
44. Zhou, J.; Chen, Y.; Zhang, X.; Zhan, W. Modelling the diurnal variations of urban heat islands with multi-source satellite data. *Int. J. Remote Sens.* **2013**, *34*, 7568–7588. [[CrossRef](#)]
45. Yan, Y.Y. The influence of weather on human mortality in Hong Kong. *Soc. Sci. Med.* **2000**, *50*, 419–427. [[CrossRef](#)]
46. Bilal, M.; Nichol, J.E.; Nazeer, M.; Shi, Y.; Wang, L.; Kumar, K.R.; Ho, H.C.; Mazhar, U.; Bleiweiss, M.P.; Qiu, Z.; et al. Characteristics of fine particulate matter (PM_{2.5}) over urban, suburban, and rural areas of Hong Kong. *Atmosphere* **2019**, *10*, 496. [[CrossRef](#)]

Disclaimer/Publisher’s Note: The statements, opinions and data contained in all publications are solely those of the individual author(s) and contributor(s) and not of MDPI and/or the editor(s). MDPI and/or the editor(s) disclaim responsibility for any injury to people or property resulting from any ideas, methods, instructions or products referred to in the content.